Loughborough
University

This item was submitted to Loughborough's Institutional Repository (https://dspace.lboro.ac.uk/) by the author and is made available under the following Creative Commons Licence conditions.

For the full text of this licence, please go to:
http://creativecommons.org/licenses/by-nc-nd/2.5/

Ultra-thin films and surface alloying of Pd on Cu(111) investigated by medium energy ion scattering

C.J. Howe[1], M.D. Cropper[1]♦, T.P Fleming[1], R.M. Wardle[1], P.Bailey[2] and T.C.Q. Noakes[2]

[1]. Department of Physics, Loughborough University, Loughborough, LE11 3TU, UK

[2]. STFC Daresbury Laboratory, Daresbury, Warrington, WA4 4AD, UK

Abstract

The structure of Pd films on Cu(111) and the alloying between the films and the substrate have been investigated by medium energy ion scattering (MEIS) using 100 keV H^+ ions. Data are presented for the $[1\bar{1}0]$ and $[11\bar{4}]$ alignments (nominal one- and three-layer alignments respectively). It is found that beyond 1 ML the Pd grows in a twinned fcc structure, the incommensurate nature of which increases the visibility of the Cu(111) substrate to MEIS. Deposition of 0.2 ML of Pd produces a structure in which Pd mostly occupies the top two layers which have interlayer distances $d_{12}=208\pm4$ pm and $d_{23}=211\pm4$ pm. Some twinning is also present in this structure. Upon annealing 1.6 ML of Pd to 600 K for 1 minute, the copper and palladium interdiffuse leaving around 0.4 ML of visible palladium. Energy plots show that there are several layers with an altered structure present over at least part of the surface. This may be due to large scale interdiffusion or alloy island formation. Incremental annealing to successively higher temperatures shows that the structural transformation begins around 500 K.

Keywords: Medium Energy Ion Scattering; Palladium; Copper; Surface Alloy; Ultra-thin Film.

♦ Corresponding author, m.d.cropper@lboro.ac.uk, +44 1509 223308, Fax: +44 1509 223986

1   Introduction

The investigation of metal-on-metal epitaxy and bi-metallic surface alloys produced by the deposition of metals is a key theme in surface science. The deposition of palladium onto Cu(111) is one example of this. It is a system that readily forms substitutional alloys [1] and it has been the subject of several experimental and theoretical investigations. A study of sub-monolayer amounts of palladium using scanning tunnelling microscopy (STM) and Rutherford backscattering spectroscopy (RBS) at room and elevated temperatures [1] revealed that palladium atoms form a disordered substitutional alloy at ascending steps. For sub-monolayer amounts of palladium, the authors observed fingered brims of palladium with a network of dark lines. They likened these lines to fcc to hcp stacking domain boundaries that had been observed in other metal-on-metal systems [2] and concluded that they were probably a strain-relief mechanism, given the mismatch in lattice parameters. All the palladium was visible to RBS in a "random" alignment, but upon heating to 523 K the palladium signal decreased indicating a complete restructuring of the surface. When palladium was deposited at this elevated temperature, at least half went subsurface.

A subsequent study [3] used angle scanned X-ray photoelectron diffraction to investigate the structure of 1 ML of palladium deposited at room temperature but with subsequent annealing at 600 K for one minute. This investigation confirmed that the system was not a simple overlayer. Several different models were tested against the data and the lowest R factor was obtained for

a model in which palladium occupied the top three layers in a random alloy in the ratios 20%:70%:20% and it was found that the Debye temperature of the surface alloy was 175 K compared with 240 K for pure copper. A subsequent modelling analysis of the system [4] made a comprehensive study of the deposition of different quantities of palladium between 0.1 ML and 1 ML and at the temperatures of 0 K, 300 K and 600 K. This reproduced the experimental observation of a surface alloy and showed that the palladium readily mixed into the top several layers; however, it did not appear to give a second layer enhancement over other layers.

The growth of palladium up to and beyond 1 ML has been investigated using reflection high energy electron diffraction (RHEED) [5] where it was found that palladium does not grow in a perfect layer-by-layer mode. At very low coverage the in-plane lattice parameter was that of bulk Cu(111) but this very rapidly relaxed to that of Pd(111), such that the transformation was complete by 1 ML. The authors proposed an alternative strain-relieving mechanism in a random surface alloy to explain this. The idea was that alloys with continuous compositional changes exhibit continuous variations in lattice parameter (Vegard's law). Thus in an incommensurate, non-pseudomorphous overlayer the lattice could simply expand laterally as more palladium was added.

Medium energy ion scattering (MEIS) [6] is a refinement of RBS that gives greater surface sensitivity and enables surface structural determinations to be made via channelling and blocking phenomena. It has several features that

make it useful for studying surface alloying; it is quantitative, it is not selectively sensitive to ordered areas of a surface as for example a diffraction method would be, and it may be used to determine the composition in a layer-specific manner. This latter point is particularly important and relies upon the correct geometrical selection of incidence and scattering angles to give sensitivity to a certain number of layers. For instance the use of a [110] type incidence direction in an fcc lattice gives full illumination of the top layer only as all atoms in subsequent layers fall within the shadow cone of the top layer. MEIS has been applied successfully to several metal-on-metal systems [7, 8, 9]

We have employed MEIS to investigate ultra-thin films of palladium between 0.2 and 4 ML deposited onto Cu(111) at room temperature and for one case following a post-deposition anneal. The aim was to investigate the structure of these films and the composition of the top three layers of the surface. In this report we show that palladium readily induces twinning when deposited on the Cu(111) and that this must be accounted for in any structural determination. We also determine the interlayer separation for selected structures and the composition of the visible layers.

2 Experimental

The experiments were performed at the UK National MEIS facility which is described elsewhere [10]. Briefly this comprises three interconnected UHV

chambers; an ion source and beamline, a scattering chamber and a surface science preparation chamber. The MEIS experiments are carried out in a scattering chamber equipped with a goniometer that has three rotational and three translational axes, and toroidal electrostatic ion analyser that disperses the scattered ions in energy whilst retaining their angular distribution. The experiments reported here employed H^+ ions nominally of 100 keV energy, but the energy could differ slightly between each experimental set-up.

The palladium on Cu(111) structures were deposited in the preparation chamber (which had a base pressure of 2×10^{-10} mbar) before transfer under ultra-high vacuum into the scattering chamber. The crystal was cleaned by cycles of sputtering with 1.4 keV Ar^+ ions followed by annealing to 725 K. Following each period of sputtering and prior to annealing, Auger electron spectroscopy (AES) was used to ensure that all traces of palladium from previous experiments had been removed. As is discussed later, twinning was induced into the crystal surface by deposition, but the sputter cycles were sufficiently prolonged to remove traces of this as is confirmed by examination of the MEIS blocking curves. AES was also employed to confirm surface cleanliness following the anneal part of the cleaning cycle. Once the crystal had cooled to 308 K, palladium was deposited from a miniature electron beam evaporation source which heated the tip of a 1 mm diameter wire that was held at +2 keV. The palladium dose was estimated using AES but then measured accurately using MEIS in a non-aligned "random" direction. To quantify the random spectra, the sensitivity of the MEIS instrument was first

determined for clean Cu(111) using the procedure outlined below for determining the number of visible monolayers in aligned spectra.

MEIS data was collected using two principal alignments; [$\bar{1}\bar{1}0$] which is a nominal one-layer illumination, and [$\bar{1}\bar{1}\bar{4}$] which is a nominal three-layer alignment. These two geometries are illustrated schematically in Figure 1(a). The data is produced in a series of two dimensional tiles which are combined to produce a display of counts versus scattering angle and ion energy. The simplest way to extract blocking curves is to correct the data for the energy lost in binary collisions ("k^2 correct") and then project the palladium peak and the copper surface peak. However, at low scattering angles the palladium and copper peaks tended to overlap, particularly for the thicker films in the three-layer [$\bar{1}\bar{1}\bar{4}$] alignment so when necessary the data was extracted by curve-fitting the peaks. Each energy channel where the peaks overlapped was fitted by Gaussians and a sigmoid for the background using a routine described elsewhere [11]. The scattering angles were calibrated by projecting the scattering from the deep bulk of the copper crystal and comparing with simulations.

Where appropriate, blocking curves were simulated using the VEGAS routine developed at FOM [12] and later modified at Warwick University [13]. Following correction for the Rutherford cross-section the data were calibrated into units of visible monolayers. This was done by comparing simulations from

6

the VEGAS routine with scattering data extracted for the clean copper surface to determine the instrumental sensitivity. The VEGAS model was constructed using the parameters determined in a previously published MEIS investigation [14] although it was found necessary to increase the in-plane surface vibrations slightly to 10 pm to fit the clean data from the [$1\bar{1}\bar{4}$] in addition to the [$\bar{1}\bar{1}0$]. This calibration procedure usually gives visibilities that are correct to 10%. Aside from a small linear count-conserving correction to account for the known variation of sensitivity of the position sensitive detector across the angular range, the data shown here have not been adjusted to fit the simulations. Where simulations are simply compared with the data neither have been scaled, however when fitting was carried out ±10% variation in visibility was allowed which is comparable with the known accuracy of the determination of visibility using this instrument and procedures. The quality of fit of simulation to data and the uncertainties in parameters so determined has been estimated using the R_{chi} method that is commonly used for MEIS [15].

3 Results and Discussion

3.1 Structure of Films with Increasing Coverage

Figure 2 shows blocking curves collected from clean and palladium covered Cu(111) in the [$\bar{1}\bar{1}0$] incident single layer illumination geometry. The number of monolayers given is relative to one complete layer of copper atoms (1.77×10^{19} m^{-2}), but this would convert to a larger number of monolayers of bulk palladium, which has a smaller atomic density. For the 0.2 ML curve this

is directly appropriate; however for the thicker films previous work [5] indicates

an incommensurate structure with the in-plane native palladium spacing. For

example, 3.4 ML of palladium measured with reference to the substrate

atomic density would be 3.9 ML relative to bulk palladium. These blocking

curves reveal much about the structure of the films using a qualitative and

semi-quantitative analysis, but they are unlikely to yield further quantitative

information using modelling. Due to the large number of atoms and variables

involved and the incommensurate and disordered nature of the thicker films, it

is likely that any parameters determined would be non-unique.

The scattering from clean Cu(111) can be seen in Figure 2(a) (filled circles).

The large dip at 90° results from the [001] blocking event, which is also a one-

layer alignment. Superimposed on this is a simulation for the clean Cu(111)

surface. In Figure 2 (b) it can be seen that the palladium blocking curves

increase in visibility with deposition but for the thicker films not all the

palladium is visible, indicating shadowing of the incident ion beam by an

ordered film. However, the visibility of the palladium is too high for a one-layer

illumination of a perfect fcc lattice and the blocking curve contains extra

structure other than that expected for a $[\bar{1}\bar{1}0]$ incidence. Looking at the 3.4 ML

curve it can be seen that in addition to the expected [001] dip at 90° there is

another near 84°. The origin of this extra dip and of the increased visibility can

be immediately appreciated by considering Figure 2(c). This shows

simulations for ion incidence in the $[\bar{1}\bar{1}0]$ and $[\bar{1}\bar{1}\bar{4}]$ directions on an ideal fcc

lattice. The $[\bar{1}\bar{1}\bar{4}]$ direction is obtained by rotating the crystal by 180° around

the surface normal from the [$\bar{1}\bar{1}$0] and would be the geometry that would occur if the film twinned. This situation is illustrated in Figure 1(b), if the normal fcc (111) crystal terminates …ABC and an fcc continuation film grows …ABCabc… then there would be regions of the film reverse-stacked …ABCacb… The new dip appearing in the [$\bar{1}$10] blocking curve is the [33$\bar{2}$] dip (nominal angle 84.24°) expected with [$\bar{1}\bar{1}$4]. Twinning the film would convert the [$\bar{1}$10] geometry into a [$\bar{1}\bar{1}$4] like incidence as can be seen by comparing Figures 1(a) and (b). That the extra dip is due to a twin type stacking fault and not others such as hcp can be seen from the simulations in Figure 2 (c). Stacking faults of the hcp type in either domain (stacked bab or bcb) do not reproduce the dip near 84° and would produce other dips within the data range. This is illustrated schematically in Figure 3, showing the blocking event that leads to the dip as a solid line and its absence in an hcp stacked film. The extra dips that would arise from hcp stacking are shown as broken lines.

From Figure 3 it can be seen that the [33$\bar{2}$] dip appearing in the [$\bar{1}$10] blocking curve requires three layers of continuous reverse ACB stacking to be present before it appears. This, it could be argued, is the minimum number of layers that could define fcc type stacking and that would constitute a true twin. The relative depth of the two dips and the visibility of the palladium gives a ratio of 0.55±0.10 for fcc continuation growth to twinned growth. The two dips are weaker than would be expected for a perfect palladium lattice, indicating disorder.

The behaviour of the copper blocking curves (Figure 2 (a)) with increasing palladium deposition is interesting. Following deposition of 0.2 ML of palladium the visibility of copper is reduced, which is consistent with a commensurate overlayer structure that shadows some of the copper substrate. The details of this structure are investigated further in the next section. However, increasing the deposition to 0.7 ML actually increases the visibility of the copper above that for the clean surface and the visibility continues to increase before saturating at around 1.6 ML of palladium. This behaviour is somewhat surprising and probably originates from two sources: the incommensurate nature of the palladium overlayer [5] and the disorder that is known [1] to be induced by the interaction of the palladium with the copper substrate. By incommensurate, we mean that there is no rational relationship between the overlayer and substrate: the film has the palladium in-plane lattice parameter, which is different from that of the copper substrate. In this case, it is to be expected that the copper substrate is fully visible, but the increase in visibility could in part be due to de-channelling of the ions by the palladium overlayer, which changes the incidence angle slightly away from that in which the top copper layers fully shadow those below.

We have carried out simulations of the effects of an incommensurate palladium overlayer with four layers on top of a Cu(111) crystal by approximating the palladium lattice parameter to be 14/13 times that of the copper and constructing a VEGAS model accordingly. From these simulations we have found that the visibility of lower layers of the Cu(111) lattice is increased due to de-channeling of the ions by the overlayer. The total

increase in visibility from this effect accounts for some of the observed increase in visibility, but caution must be exercised in quantifying this since the VEGAS routine was not designed to handle incommensurate systems such as this. However, based on this modelling we could estimate that about half of the increased visibility results from de-channelling and about half from disorder. An apparent shift in the [001] blocking dip for the copper in the two higher coverages of palladium, may be due to a small increase in the surface interlayer distance or an effect of the de-channelling.

Two other possible sources of this increased visibility can be eliminated. Firstly, although there is published evidence of intermixing between copper and palladium in very thin layers [1, 3] the extra visibility seen above 1ML here cannot be caused by copper diffusing up through the palladium film as these copper blocking curves do not show evidence of twinning. The second point is that though it is reported that at very low coverage palladium substitutes the copper atoms and displaces them to a capping layer [1], the 3.4 ML palladium film investigated here is not covered with a copper overlayer. The evidence for this is the energy projection taken for a $[\bar{1}\bar{1}4]$ incident direction and a [110] outgoing direction (nominal one-layer sensitivity) shown in Figure 4 in comparison with that for clean copper. This projection does not show two separate copper layers as would be seen if here was a copper cap. Nor does the energy projection show evidence of large scale copper diffusion into the palladium: the leading edge of the copper surface peak is displaced to lower energy by the 600 eV expected for a 4 ML

overlayer of palladium. The thickness of 4 ML of (111) oriented palladium would be 0.9 nm and the total path length of the ions is increased by the angle from normal of 35.26° for both the ingoing and outgoing directions, giving a total path in the palladium of 2.2 nm. The calculated inelastic energy loss for hydrogen ions in palladium is 265 eV/nm [16], giving an expected shift in energy of the copper surface peak of 583 eV.

3.2 Structure of 0.2 ML of Palladium on Cu(111)

It is known that at very low coverage, the structure formed by palladium on Cu(111) is commensurate [5]. This makes it possible to determine several structural parameters by comparing the data with simulations. The 0.2 ML deposition falls into this commensurate regime and therefore has been analysed in further detail. It can be seen from Figure 2 that this coverage differs from the higher ones as the visibility of the copper is lower than that for clean copper, indicating that commensurate palladium atoms are shadowing copper substrate atoms.

The 0.2 ML structure was simulated by using large VEGAS models in which some copper atoms in various layers were randomly substituted by palladium atoms in such a way as to keep the total number of palladium atoms the same as had been determined by non-aligned MEIS analysis. For the models presented here, the atomic vibrations were kept the same as those determined for clean Cu(111), but the influence of adjusting these parameters

has been investigated and was found to make no significant difference to the conclusions. The parameters that were varied were the palladium occupation of the top three layers, the effect of any twinning, and the top two interlayer distances.

Before considering the results of the simulations, some insight into the surface structure can be obtained by observing the features present in the data shown in Figure 5. Firstly, the environment occupied by the palladium atoms is similar to that occupied by copper as evidenced by the similarity of the blocking curves. There are no obvious deviations from fcc structure and there are no major shifts in blocking dip angles between the copper and palladium data suggesting that there are no large distortions induced by the presence of the larger palladium atoms.

Secondly, it is clear that the palladium is not completely restricted to a single top layer. There are two pieces of evidence for this; the relative visibility of the $[\bar{1}\bar{1}0]$ and $[\bar{1}\bar{1}\bar{4}]$ palladium data and the dips in each alignment. The visibility of the palladium in the one-layer $[\bar{1}\bar{1}0]$ alignment is slightly lower than that in the three-layer $[\bar{1}\bar{1}\bar{4}]$ alignment implying that some palladium atoms are in layer two and/or layer three and are being partially shadowed by layer one atoms. Whether this shadowing is by copper or other palladium atoms cannot be distinguished from the data. The palladium data also shows the one-layer dips [001] (nominally at 90° for an ideal lattice termination) in the $[\bar{1}\bar{1}0]$ data and

[11$\bar{1}$] (nominally at 74.21°) in the [$\bar{1}$1$\bar{4}$] data, where the outgoing ions scattered from palladium atoms are blocked by atoms in layers nearer the surface.

The third feature to note from the data in Figure 5 is that there is less palladium in the third layer than in the second layer. This can be seen by looking at the [33$\bar{2}$] blocking dip (nominally at 84.24°) in the [$\bar{1}$1$\bar{4}$] data, which is a two-layer dip, requiring occupation of the third layer to be present. It is clearly visible in the copper data but in the palladium data it may be present, but to a level comparable with the noise in the spectrum. Allowing a small amount of palladium to be in the third layer improves the fit as discussed below, but the improvement in fit does not meet the normal criteria for significance [15].

A fourth feature visible in the data is the lower angle shoulder on the [001] blocking dip in the Cu data with [$\bar{1}$1$\bar{0}$] incidence. Reference to Figure 2 suggests that this may be due to some twinning already present in the surface. This effect has been included in the simulations of the data. The broken line in the top two panels of Figure 5 show the effect of twinning the top two layers of the crystal. It can be seen that this does produce a dip [33$\bar{2}$] near 84° that would make a shoulder on the data, but that such a twin could drastically change the shape of the [$\bar{1}$1$\bar{4}$] data. Investigations of the effect of

different fractions of twining indicate that provided the fraction of twining is less than 25%, little change to the [$\bar{1}\bar{1}4$] data will be immediately noticeable. As mentioned earlier, previous STM work [1] has imaged misfit dislocations in the fringes of palladium islands in sub-monolayer coverage. This was said to be reminiscent of fcc to hcp domain boundaries seen in Ag on Pt(111) [2]. Based on the evidence shown here, these would now appear to be fcc to fcc-twin boundaries; that is a boundary between ABC and ACB stacking. A stacking fault between the second and first layer to give top-layer only occupation of the hcp site would not produce the dip near 84° seen in our data, as can be seen from the dotted line in Figure 5. As we have a lower coverage than was imaged in STM our islands will be smaller and hence a larger fraction of them lies on the faulted brim. The driving force for these stacking faults is most likely the need to relieve the strain induced by the presence of the larger palladium atoms within the copper layers. This strain would locally shift a layer by half of a lattice spacing into an hcp site seeding the twin. A network of such partial dislocations has been imaged in STM [17] on another system.

Figure 5 shows the results of VEGAS simulations superimposed on the data. The solid black line is from a model which the first layer is 9% palladium and 91% copper by atom, the second layer is similarly 9% palladium and 91% copper and the third layer 2% palladium and 98% copper. This was found to give the best fit to the data, and reproduces adequately both the visibility and the relative strength of the one-layer and two layer dips. To reproduce the

shoulder on the low scattering-angle side of the [001] dip in the Cu [$\bar{1}\bar{1}$0] data, it was found necessary to include 15% reverse stacking (twinning) of the top two layers. Also shown in Figure 5 are the results of simulations of an alternative model in which all the palladium is in the second layer (grey line). It can be seen that this second model produces dips in the palladium blocking curve that are too large and so this model can be eliminated. All possible distributions of the palladium between the top three layers have been tested and the near-bilayer model outlined above is favoured. The interlayer distances that were determined from these simulations were d_{12}=208$\pm$4 pm and d_{23}=211$\pm$4 pm, neither being significantly different from the 208.7 pm interlayer distance of Cu(111).

3.3 The Effect of Annealing on Palladium Films

An important theme in published work on the structure of palladium on Cu(111) has been the effect of a post-deposition low temperature anneal. For this reason we have investigated the effect of a one-minute 600 K anneal and then sequential annealing to successive temperatures on palladium on Cu(111) using MEIS.

The results of the first experiment, the annealing of the 1.6 ML deposition, are shown in Figure 6. The left-hand panel shows the palladium and copper blocking curves for the one-layer [$\bar{1}\bar{1}$0] incidence geometry and the right hand shows them for the three-layer [$\bar{1}\bar{1}\bar{4}$]. Notice that the [$\bar{1}\bar{1}$0] palladium visibility

is much reduced from the non-annealed sample shown in Figure 2, and for both alignments is well below the nominal coverage of 1.6 ML. This suggests that the surface has re-arranged to cause shadowing of palladium atoms. This shadowing is more than would be expected from an improvement in order of a monolayer or bilayer and indicates that some of the palladium is hidden in layers below the top three. That palladium is not confined to the top two layers is confirmed by the [$\bar{1}\bar{1}4$] palladium blocking curve, where the [11$\bar{1}$] (nominally 74.21°), [33$\bar{2}$] (nominally 84.24°) and probably [22$\bar{1}$] (nominally 90°) dips are apparent. The presence of the [11$\bar{1}$] requires palladium to be in the second layer, the [33$\bar{2}$] the third layer and the [22$\bar{1}$] the fourth layer. Care must be taken with the latter dip as any twinning would put the [001] here. Put together, the change in visibility and appearance of dips indicate that the surface has been restructured significantly by quite a low temperature anneal.

The blocking curves shown in Figure 6 show significant evidence of twinning in the surface, not just in the palladium blocking curves but also in those from the copper. There are two pieces of evidence for the twinning, the first of which is the relative visibility of the [$\bar{1}\bar{1}0$] and [$\bar{1}\bar{1}4$] blocking curves. For both elements, the visibility in each geometry is more similar than would be expected for a simple fcc termination. The second piece of evidence for twinning is the [33$\bar{2}$] dip (nominal 84.24°) which is clearly visible in both the palladium and copper [$\bar{1}\bar{1}0$] blocking curves. This is conclusive evidence that a twinned structure has been formed by the annealing that involves both palladium and copper. That there is a significant amount of copper involved in

the twinned structure can be seen from the strength of the [33$\bar{2}$] dip in the [$\bar{1}\bar{1}$0] blocking curve. Strictly, the presence of this dip requires copper atoms to be in a layer below two reverse stacked layers, but the low visibility of the palladium suggests that these two upper layers cannot be dominated by palladium.

In considering how large a restructuring of the surface structure there has been, an energy spectrum can be informative. Figure 7 shows a spectrum collected using the same geometry as in Figure 4, that is [$\bar{1}\bar{1}\bar{4}$] in, [110] out. The spectrum for the as deposited 1.6 ML shows two surface peaks, one for copper and one for palladium. Upon annealing, the surface peak for palladium decreases significantly in intensity as can be seen from Figure 7(b). The spectrum for the annealed surface shows three distinct peaks; the palladium peak is at highest energy, the true copper surface peak at 99.4 keV and another, deeper, peak can be seen at 98.5 keV. This latter peak is due to scattering from sub-surface atoms that have been made visible by the lattice disruption. That is, visible copper atoms that are below a significantly altered layer. The energies of these peaks were determined by fitting asymmetric Gaussians to the peaks, together with a sigmoidal background. From this fit, the energy separation of the copper surface peak and the extra peak in this geometry is equivalent to 9 layers, based on an average loss of 200 eV/nm for the palladium/copper combination [16]. This indicates that there is altered structure present on the surface that is several layers thick.

Given that it is clear that the palladium has been re-distributed significantly by the annealing process, it would be interesting to investigate the layer-by-layer composition starting at the surface. It is common to use the three-layer, two-layer and one-layer dips in the $[\bar{1}\bar{1}4]$ alignment to obtain layer-by-layer compositions [18]. The counts at the bottom of the three-layer dip enable the fraction of each element in the top three layers to be determined, then the two layer dip does the same from the top two layers and so on. It is then a matter of straightforward arithmetic to determine the composition of each layer. However, the reliability of this method relies on there being just one double-alignment geometry, not the two that would occur in the presence of twinning. Therefore, it was impossible to safely determine the layer-by-layer composition using this or similar methods [19]. However, the variation of composition with depth may be determined by full simulation of the blocking curves, including the effect of twinning. In performing such an analysis it is important not to over interpret as some of the parameters will be correlated, given that it is necessary to average several models representing what may be two or more local structures on the surface.

To investigate the distribution of the palladium in the surface layers, large VEGAS models were created for two domains, twinned and non-twinned. For these models the fraction of palladium in each layer, the top-two interlayer distances, the fraction of the surface that is twinned and the thermal vibrations were adjusted to give a good fit to the data. These model fits are shown In Figure 6 as solid lines, superimposed on the data. The first stage in the

modelling was to determine the top two interlayer distances using an R-factor approach modified to cope with the problem that the R-factor would be dominated by total visibility rather than the angular position of the dips in this complicated multi-parameter situation. A scaling parameter was used to minimise the effect of visibility and the fit was limited to the one and two-layer blocking dips in the $[\bar{1}\bar{1}\bar{4}]$ spectrum, as these were least likely to be distorted by the presence of twinning. Using this approach, the top interlayer spacing was found to be expanded by 2.5±2.0% over the ideal fcc termination, and the second interlayer spacing was contracted by 4±2%. It is not known if the structure that has been formed by annealing is commensurate or incommensurate, or a mix of the two but applying these values to an in-plane repeat distance equal to that of clean Cu(111) would produce a top layer spacing of d_{12}=214±4 pm and a second layer spacing, d_{23}=201±4 pm.

The next stage in the simulation was to determine the other parameters that strongly affect visibility. These parameters were varied together to obtain a minimum in R-factor without scaling. The main difficulty in this procedure was imitating the high visibility of the copper signal. The visibility in the $[\bar{1}\bar{1}\bar{4}]$ signal is almost the same as for clean Cu(111) despite the twinning and presence of palladium and the visibility of the $[\bar{1}\bar{1}0]$ is not much lower. The only method that was found to simulate this was to increase the thermal vibrations for the top four layers to around 13 pm, compared with 10 pm for the surface layer of clean Cu(111) and 8 pm for the bulk. This probably actually reflects static disorder induced by the presence of the larger palladium atoms rather than

thermal effects as the two of these are difficult to distinguish in MEIS. Previous STM studies of palladium inclusion into the top layer of Cu(111) revealed disorder [1].

The model fit shown in Figure 6 used a fraction of twinning of 30% and fractions of palladium in the first, second and third layers of 16%, 13% and 7% respectively. A good fit was obtained if subsequent layers also had 7% palladium content, but the data is rather insensitive to the exact value of this as these layers are mostly shadowed. The main parameters strongly correlate so their determination may not be a unique solution. The precision of the determination of the twinning fraction is $\pm 10\%$ and the precision of the determination of the composition of the second layer $\pm 3\%$. The composition of the top layer is more problematic as it does not generate dips and therefore is hard to distinguish from disordered and incommensurate material. However it is less than 23% palladium and more than 12%. It should be borne in mind that these values are averages across whatever structures might be present.

In their photoelectron diffraction work, de Siervo et al obtained values of $d_{12}=220\pm10$ pm and $d_{23}=205\pm30$ pm, in agreement within error with our values assuming an in-plane lattice parameter equal to that of Cu(111), and they obtained similar values to ours for the surface vibrational amplitude. However, their model required the majority of the palladium to be in the second layer which is incompatible with our MEIS results. Simulating their model using

VEGAS overstates the palladium visibility by around a factor of 2 and understates the copper visibility. However, care must be taken in making direct comparisons as it is difficult to reproduce experimental conditions. The experiment here started with more palladium on the surface but the heating and cooling rates may have been slower. De Siervo et al did not explicitly state whether they tested for twinning, but the planar projections of their XPD data shows three-fold symmetry. Our palladium films have been shown to twin readily so the difference in observed behaviour may rest upon the precise growth conditions or the detailed nature and history of the single crystal substrate, including such parameters as step density.

The annealing of a palladium film was repeated for several temperatures to observe the progression of the interdiffusion. Approximately 1 ML of palladium was deposited onto Cu(111) at 300 K and MEIS data were collected in the $[\bar{1}\bar{1}\bar{4}]$ incidence geometry. The crystal was then heated briefly to various, successively increased temperatures and palladium blocking curves obtained, (shown in Figure 8). Again the possibility of twinning has prevented a straight forward determination of the layer-by-layer composition, but several features are visible in the raw data. The as-deposited spectrum contains dips, again showing that the palladium is not restricted to a single layer. Both the $[11\bar{1}]$ (nominal 74.21°) and [001] (nominal 90°) one-layer dips arising from twinning are present, but the palladium structure is poorly ordered as these dips are weak. Upon heating to 425 K, little has changed but after heating to 500 K the amount of palladium visible in the top three layers has started to fall. This

must, in fact, be close to the transition temperature. In the 500 K curve the [11$\bar{1}$] one-layer dip (nominal 74.21°) has become more pronounced, suggesting that the non-twin orientation is starting to be more prevalent or that disorder has decreased. There is also a weak [33$\bar{2}$] dip (nominal 84.24°) which arises when third layer occupation is taking place. Despite the difference in starting composition and the different heating regime, the blocking curve collected after heating to 600 K is virtually identical to that obtained from the previous annealed film and solves to give similar layer-wise composition. That is, much of the palladium is no longer visible, indicating interdiffusion and the presence of one- two- and three layer dips reveals that the visible palladium is distributed through all three/four visible layers.

The findings for the effect of low-temperature anneals are complex and interpretation needs some care. The main features are that extensive twinning is present in both the palladium and copper related features, the palladium visibility is greatly reduced by the annealing, and that there is evidence of the presence of a modified structure extending many layers. Two scenarios may be constructed to explain the features that are seen, but unfortunately they may not be directly distinguished using MEIS.

The first scenario is that the annealing has caused the palladium to interdiffuse with the copper forming an extended surface alloy, reducing the visibility of the palladium and inducing twinning into the copper surface. This is

an extreme version of the model proposed by de Siervo et al [3] and would be supported in part by the simulations of Canzian et al [4] which show a continual mixing of the palladium into the Cu(111) surface at 600 K. In this model the palladium visibility would fall as it diffuses into the copper and the surface layers become dominated by copper. The presence of the larger palladium atoms would produce stress, which could be alleviated by the formation of a partial dislocation whereby locally a part of a plane shifts onto an hcp site and causes the twin. Such a large scale interdiffusion would be surprising, given the activation energy for the diffusion of palladium in copper of 2.36 eV [20] which would seem to preclude significant diffusion at 600 K. There have been reports of interdiffusion between palladium and copper films [21] but not to the extent that would be required here in the short experimental timescale. Interdiffusion in thin films is likely to take place more quickly than in the bulk as the film is more loosely packed. Hence in our experiments we could be seeing the copper atoms diffusing up into the palladium overlayer, rather than the palladium diffusing down into the bulk. However, for such a large scale disruption to be responsible for the effects seen in MEIS would be remarkable.

A second explanation for the observed effects would be for the annealing to activate surface diffusion of the palladium and some copper into islands. This island formation would reduce the visibility of the palladium by shadowing of lower layers in the islands by upper layers. It would be highly likely that these islands would grow in both stacking directions, giving the observed palladium twinning. In this scenario, the extra surface-like peak in the energy plots would

be due to the copper surface being visible below high islands that would have either a disrupted, twinned structure or were incommensutrate by having a larger in-plane lattice constant. This latter scenario is more likely than the first and if this is what occurs then it must be borne in mind that the outcomes of the VEGAS simulations average over two different structures; islands of palladium copper alloy and a surface alloy in the terraces in between.

4   Summary

MEIS has been employed to investigate the structure of palladium films on Cu(111) and the alloying between the films and the substrate. It is found that beyond 1 ML the palladium grows in a twinned fcc structure, the incommensurate nature of which increases the visibility of the Cu(111) substrate to MEIS. The structure of 0.2 ML of palladium has been investigated in more detail and is best fitted by a model in which equal amounts of palladium occupies the top two layers, with some third layer occupation. 15% twinning of the top two layers gives the best fit to data, and the top two interlayer distances are $d_{12}=208\pm4$ pm and $d_{23}=211\pm4$ pm. Upon annealing 1.6 ML of palladium to 600 K for 1 minute, the copper and palladium interdiffuse leaving around 0.4 ML palladium visible. This visible palladium is distributed throughout the top three layers, but no particular second layer enhancement is seen. Significant twinning is observed in the copper blocking curves which may be explained by significant interdiffusion of the copper into the palladium film. Energy plots show that the restructuring of the surface happens over several layers for at least part of the surface. These three

observations may be explained either by an energetically unlikely interdiffusion of copper and palladium over many layers or by the formation of palladium/copper alloy islands combined with some incorporation into the copper surface layers to induce twinning. The top interlayer distance for this structure is expanded by 2.5±2.0% and the second contracted by 4.0±2.0% compared with an ideal fcc termination.

5 Acknowledgements

6 References

[1]   A. Bach Aaen, E. Lægsgaard, A.V. Ruban, I. Stensgaard, Surface Science 408 (1998) 43.
[2]   H Brune, H. Röder, C. Boragno, K. Kern, Physical Review B 49 (1994) 2997
[3]   A. de Siervo, E.A. Soares, R. Landers, T.A. Fazan, J. Morais, G.G. Kleiman, Surface Science 505 (2002) 215.
[4]   A. Canzian, H.O. Mosca and G. Bozzolo, Surface Science 551 (2004) 9.
[5]   R. Panagio, A. de Siervo, E.A. Soares, H.-D. Pfannes, R. Landers, Surface Science 560 (2004) 27.
[6]   J.F. van der Veen, Surface Science Reports 5 (1985) 199.
[7]   M.T. Butterfield, M.D. Crapper, T.C.Q. Noakes, P. Bailey, G.J. Jackson and D.P. Woodruff, Physical Review B 62 (2000) 16984.
[8]   M.D. Cropper, T.C.Q. Noakes, M.T. Butterfield, P. Bailey, Surface Science 594 (2005) 212
[9]   P.C. Dastoor, D.J. O'Connor, D.A. MacLaren, W. Allison, T.C.Q. Noakes, P. Bailey, Surface Science 588 (2005)101.
[10]   P. Bailey, T.C.Q. Noakes, D.P.Woodruff, Surface Science 426 (1999) 358.
[11]   A.G. Trant, T.E. Jones, J. Gustafsson, T.C.Q. Noakes, P. Bailey, C. J. Baddeley, Surface Science 603 (2009) 571.
[12]   R.M. Tromp and J.F. van der Veen, Surface Science 133 (1983) 159.
[13]   XVegas Version 132, Paul Quinn, (2005).
[14]   K.H. Chae, H.C. Lu, T. Gustafsson, Physical Review B 54 (1996) 14082.

[15]   T.C.Q. Noakes, P. Bailey, D.P. Woodruff, Nuclear Instruments and Methods in Physics Research B 136-138 (1998) 1125.

[16]   J. F. Ziegler, SRIM – The Stopping and range of Ions in Matter (2008), www.SRIM.org.

[17]   V. Fournée, J. Ledieu, T. Cai, P. A. Thiel, Physical Review B 67 (2003) 155401

[18]   T. G. Owens, T. E. Jones, T. C. Q. Noakes, P. Bailey, C. J. Baddeley, Journal of Physical Chemistry B 110 (2006) 21152.

[19]   C. J. Baddeley , L. H. Bloxham, S. C. Laroze, R. Raval, T. C. Q. Noakes, P. Bailey, Journal of Physical Chemistry B 105 (2001) 2766

[20]   J. Askill, Radioactive Tracer Diffusion data for Pure Metals, in: D. R. Lide, H. P. R. Frederikse (Eds.), CRC Handbook of Chemistry and Physics 75th Edition, CRC Press., Boca Raton, 1995, pp. 12-172-12-179.

[21]   J. M. Heras, L. Viscido, G. Wedler and D. Borgmann, Surface and Interface Analysis 16 (1990) 493

Figure 1: A schematic of the scattering geometries used. (a) If the fcc (111) surface terminates in layers designated …CABC then the [$1\bar{1}\bar{4}$] incidence illuminates the three surface layers with subsequent layers shadowed. In the data range presented here there are three main outgoing blocking dips due to the [$11\bar{1}$], [$33\bar{2}$] and [$22\bar{1}$] crystallographic directions, which allow scattering from one layer, two layers and three layers respectively. The [$\bar{1}\bar{1}0$] incidence illuminates only the top layer fully and in the data range there is one principal blocking dip due to the [001] direction. (b) When a stacking fault reverses the direction of stacking to produce the "twin" …ABCbac sequence, the previous [$1\bar{1}\bar{4}$] incidence is reduced to a one-layer geometry and the previous [$\bar{1}\bar{1}0$] incidence becomes a three-layer geometry.

Figure 2: Blocking curves collected from clean Cu(111) and following the deposition of 0.2, 0.7, 1.6 and 3.4 ML of palladium. The measurements used the [$\bar{1}\bar{1}0$] incident geometry. Panel (a) shows the copper surface peak, panel (b) that from the palladium and panel (c) the results of simulation of [$\bar{1}\bar{1}0$] incidence on: the fcc lattice that may be described …ABC; the mirror geometry that would arise in the presence of twinning and may be described …CAB; the two domains of hcp stacking that could arise, …BAB and …BCB.

Figure 3: The blocking event near 84° for the [$\bar{1}\bar{1}0$] geometry is characteristic of a reverse stacked "twin". If the fcc (111) crystal terminates …ABC then the twin would stack …ABCbac as indicated on the left, the blocking event being shown by a solid line. The two possible domains of hcp stack …ABCbab and

…ABCbcb as shown. They do not produce the observed dip, indicated by solid lines, but would put other dips into the data range shown by broken lines.

Figure 4: An energy projection with no kinematic correction taken for $[\bar{1}\bar{1}4]$ incidence and [110] take-off being sensitive to about one and a half layers. It shows the spectrum from a clean Cu(111) surface (broken line) and one covered with 3.4 ML of palladium.

Figure 5: MEIS data from 0.2 ML of palladium deposited onto Cu(111) for both the one-layer $[\bar{1}\bar{1}0]$ and three-layer $[\bar{1}\bar{1}4]$ incidence directions. The scattering from the copper atoms is denoted by triangles and that from the palladium by circles. Superimposed are the results of simulations using two different models: palladium atomic concentration in the top three layers 9%, 9% and 2% (black line), and all the palladium in the second layer (grey line). Included in the simulation is 15% twinning of the top two layers. The simulation of the fully twinned surface is shown as a broken line, and for comparison the simulation of a top layer stacking fault only is shown dotted.

Figure 6: MEIS data for both the one-layer $[\bar{1}\bar{1}0]$ and three-layer $[\bar{1}\bar{1}4]$ incident geometries from the structure formed by annealing 1.6 ML of Pd on Cu(111) at 600 K for 1 minute. The copper and palladium data for two incident alignments are shown together with the best fit from a VEGAS simulation (solid line). The details of the model are given in the text.

Figure 7: Energy projections with no kinematic correction taken for [$\bar{1}\bar{1}\bar{4}$] incidence and [110] take-off showing the spectrum from (a) 1.6 ML of palladium as-deposited on Cu(111) and (b) the same surface after a one minute anneal to 600 K.

Figure 8: Palladium blocking curves extracted using the three-layer [$\bar{1}\bar{1}\bar{4}$] incident geometry from 1 ML of palladium on Cu(111) at (a) 300 K and following sequential anneals to (b) 425 K, (c) 500 K and (d) 600 K. The data shows the reduction in visibility as interdiffusion occurs and the development of blocking dips as palladium atoms become shadowed.
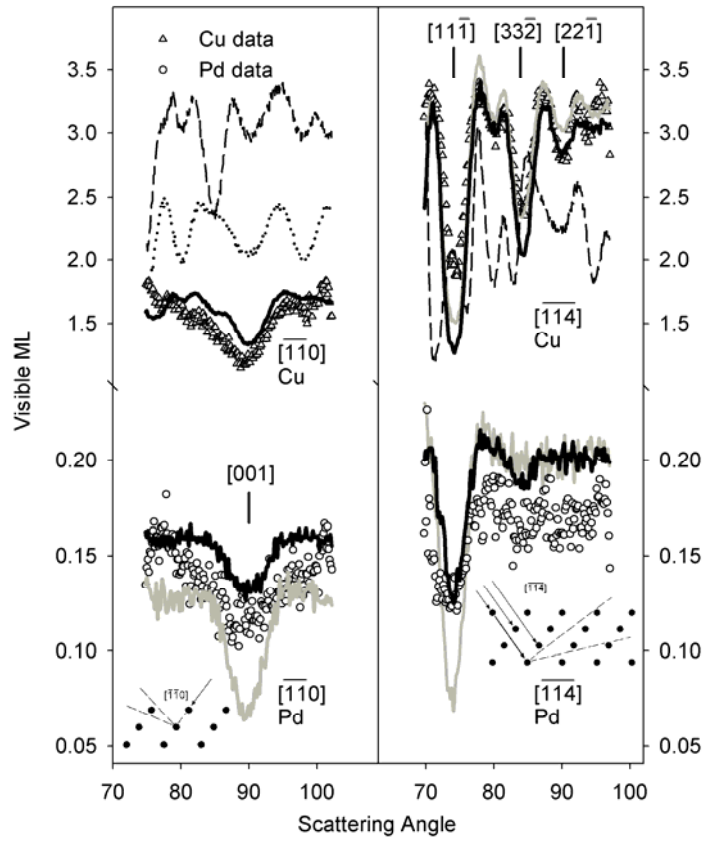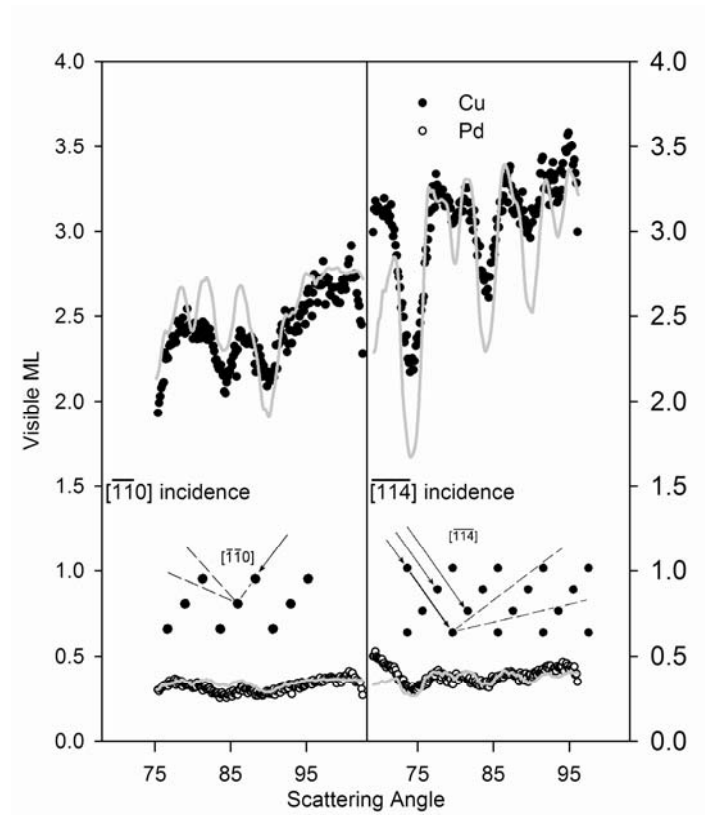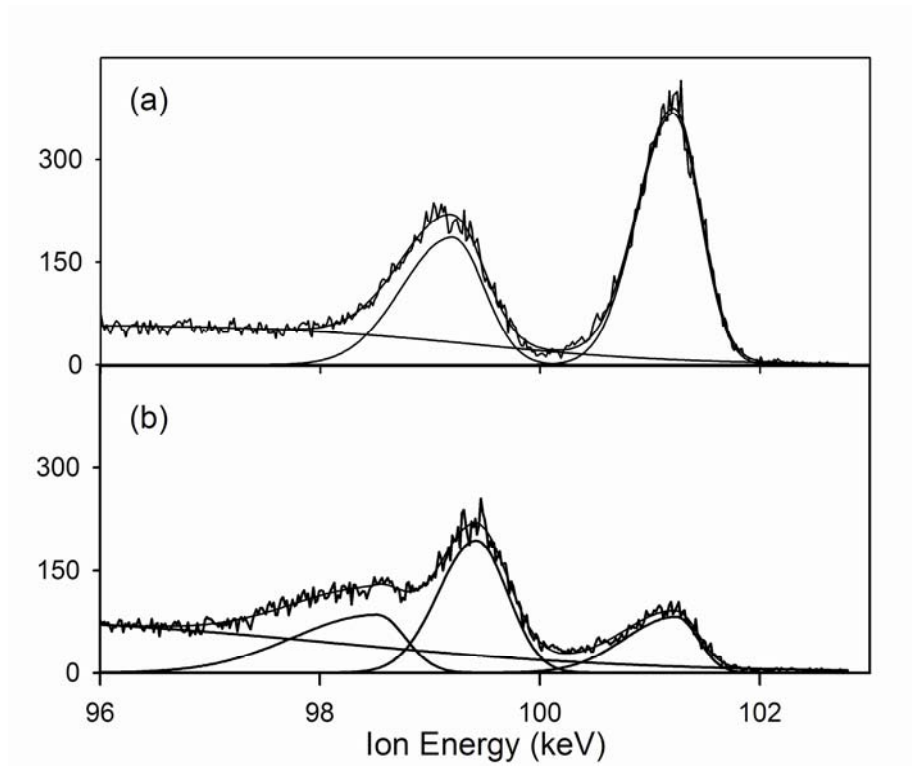
Figure 1
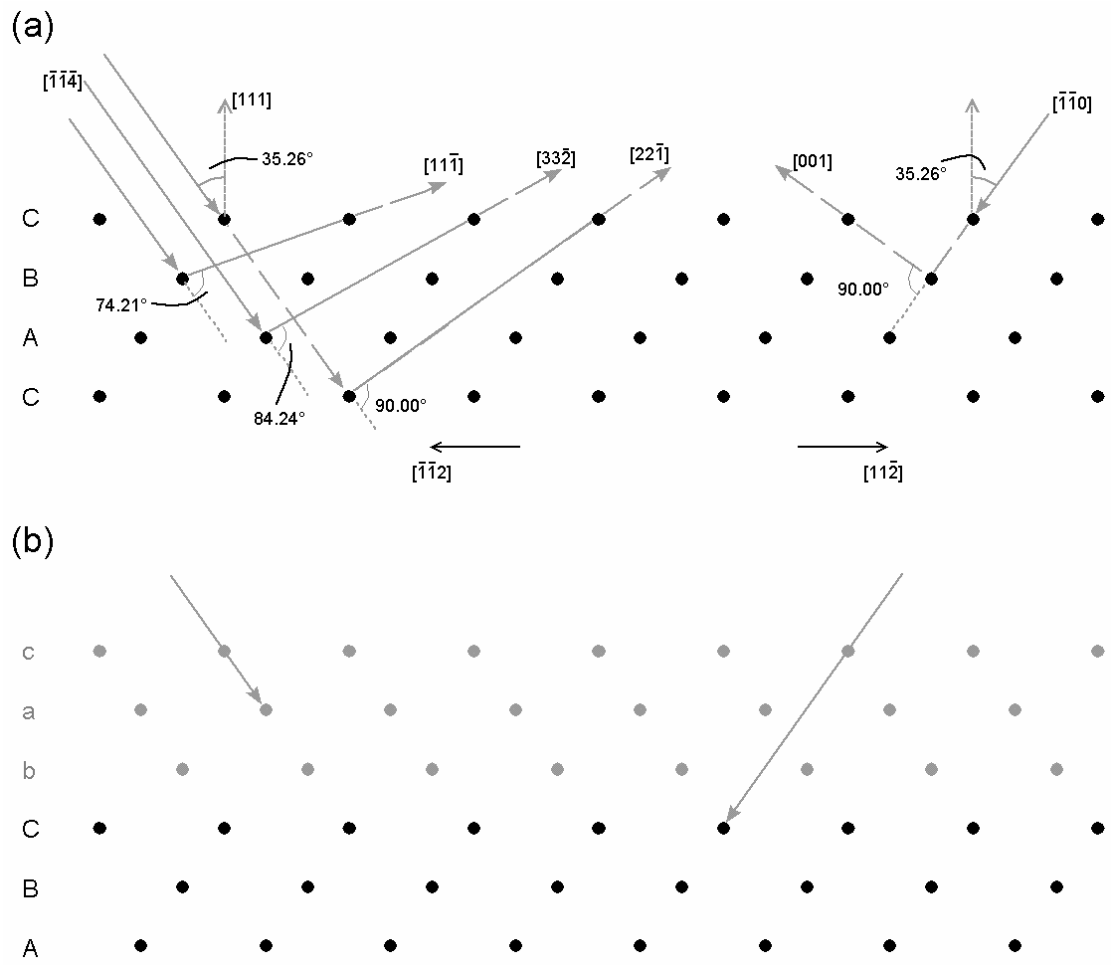
Figure 2
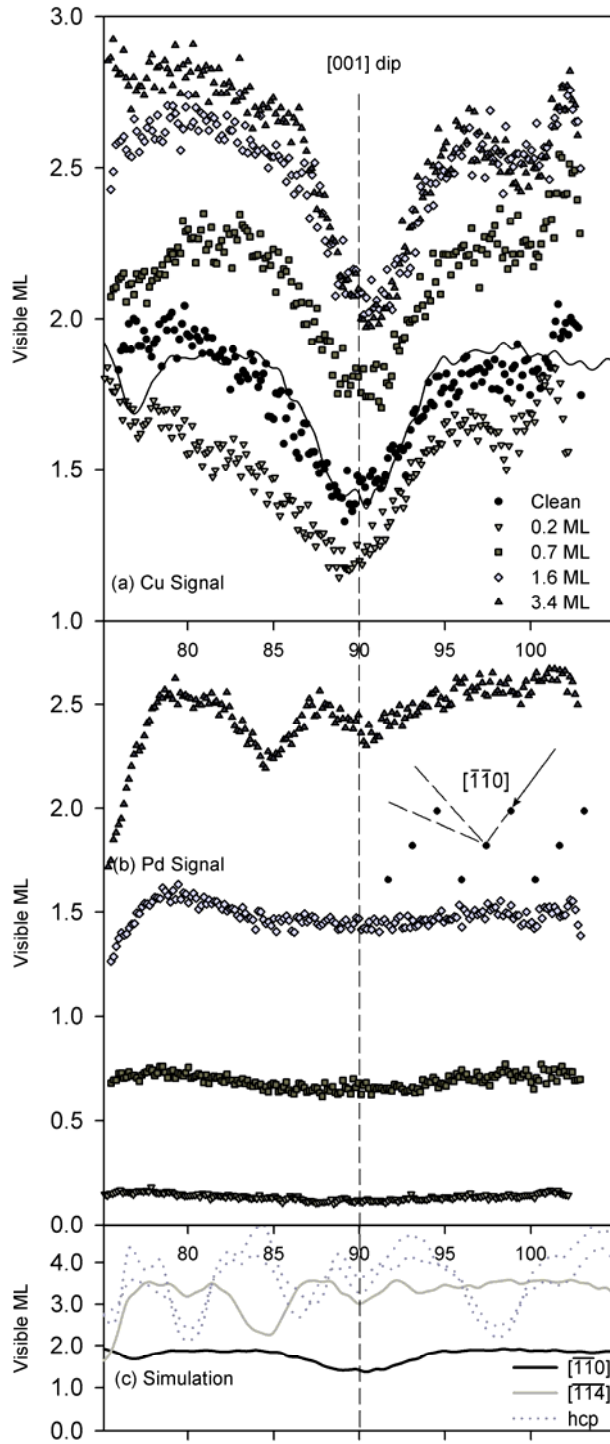
Figure 3
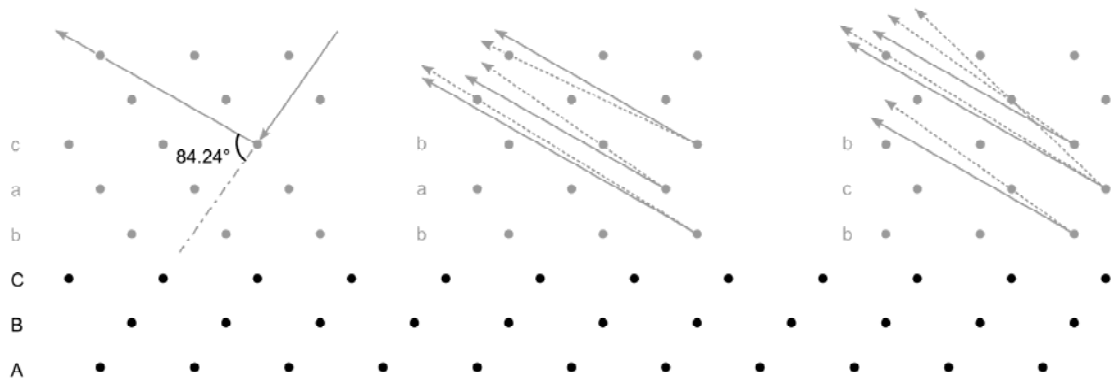
Figure 4
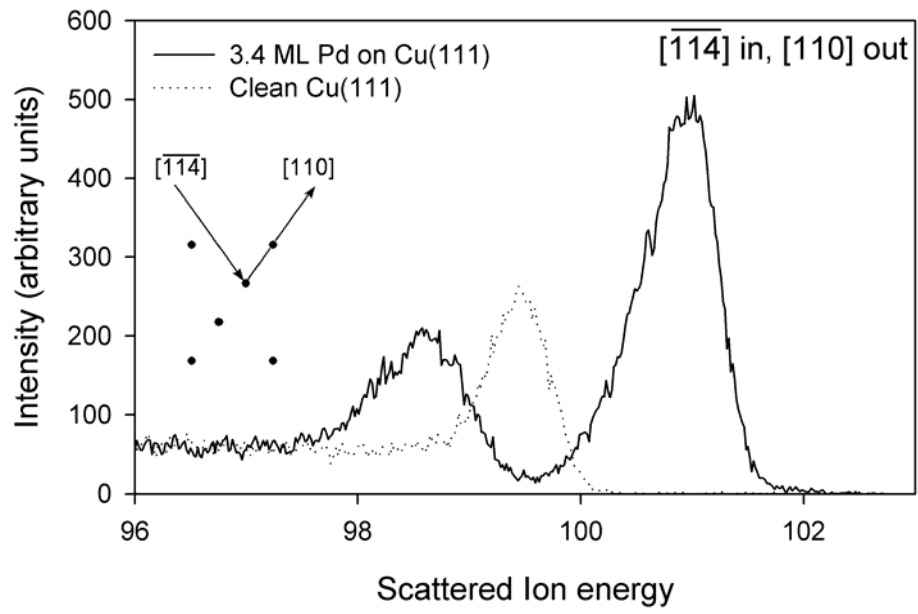
Figure 5

Figure 6

Figure 7

Figure 8